



## Research paper

# Facile and controllable synthesis of iron nanoparticles directed by montmorillonite and polyvinylpyrrolidone



Mingde Fan\*, Lijie Zhang, Ruizhe Wang, Haozhe Guo, Shiyu Jia

School of Ecology and Environment, Inner Mongolia University, Hohhot 010021, China

## ARTICLE INFO

## Keywords:

Iron nanoparticle  
Montmorillonite  
Polyvinylpyrrolidone  
Sodium borohydride  
Card-house structure

## ABSTRACT

Porous host-hybridized metal nanoparticles are of great potential in sorption and catalysis related processes. The objective of this study was to synthesize property-controllable iron nanoparticles in montmorillonite and polyvinylpyrrolidone involved borohydride reduction system. In this system, mixed primary and secondary iron nanoparticles were readily generated. These resulting nanoparticles displayed an  $\alpha$ -Fe@iron-oxide@polyvinylpyrrolidone core-double-shell architecture, in which the oxide shells protect the  $\alpha$ -Fe cores from thorough oxidation in essential. In hybridization process, a polymer barrier was developed on the clay mineral surfaces. Due to the barrier-related steric hindrances and/or the alkaline pH-derived electrostatic repulsions, the clay mineral particles built a card-house flocculation structure, which can be converted to a semi-card-house form in dry products by suitable washing and drying treatments. The binding of the polymer to the iron and clay mineral surfaces would be mainly through hydrogen bonding. In general, the card-house pores and polymer layers made the hybridized iron nanoparticles much smaller and more dispersed than their bare counterparts. Specifically, by adjusting the molar mass and concentration of the polymer and the reductant amount, the hybridized iron nanoparticles could be further optimized. This synthesis route is carried out in situ under ambient temperature and atmosphere, greatly simplifying the process for iron nanoparticles preparation.

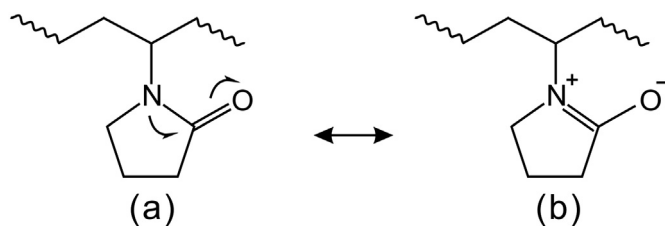
## 1. Introduction

As a naturally occurring porous clay mineral material, montmorillonite (Mt) has become an attractive host for generating various nanoparticles in terms of its unique layered structure, surface charge distribution, and cation-exchange, intercalation and swelling behaviors. In an aqueous dispersion under certain conditions of pH and electrolyte and clay mineral concentration, Mt (except  $\text{Li}^+$ -saturated form) generally forms particles or tactoids rather than thoroughly exfoliated individual unit layers (Schramm and Kwak, 1982; Carrado and Xu, 1998; Séquaris et al., 2002). These clay mineral particles arise from the uneven stacking of Mt layers along the [001] direction with heterogeneous charged edge and face surfaces. The charges on the face are permanently negative due to the isomorphous substitutions in the unit layers, whereas the edge charges due to hydroxyl groups are strongly pH dependent. The isoelectric point of the edge is commonly taken as  $\sim$ pH 7 (Ganley and Van Duijneveldt, 2015), though this value has also been reduced to as low as pH 4.0 (Pecini and Avena, 2013) or 3.5 (Thomas et al., 1999). Thus, by manipulating the dispersion pH and consequently the edge charge property of clay mineral particles, a card-house flocculation structure (taking clay mineral particles as building

blocks) could be formed mainly through two opposite electrostatic interactions. First, at the  $\text{pH} <$  the edge isoelectric point, the card-house is possible through the electrostatic attractions of the positively charged edges to the negatively charged faces (i.e., edge-to-face attractions) of Mt particles (Van Olphen, 1951). Second, at the  $\text{pH} >$  the edge isoelectric point, all the surfaces of Mt particles are negatively charged and the interparticle electrostatic repulsions (i.e., edge-to-edge, edge-to-face, and face-to-face repulsions) are dominant, also leading to the card-house structure (Benna et al., 1999; Ramos-Tejada et al., 2001). Such structure contains integrated micro-, meso- and macropores, the former one being mostly derived from the intraparticle or interlayer pores yet the latter two, the interparticle pores (Chen et al., 1995; Yuan et al., 2006a). These pores, for their spatial confinement effects on the balance of nucleation, growth, and agglomeration of nanoparticles, can be used as nanoreactors to fabricate a large variety of nanoparticles (Yuan et al., 2009; Ontam et al., 2012; Dutta et al., 2015; Saikia et al., 2016). Moreover, in the card-house structure the macro- and meso-porosities are typically more enhanced than the microporosity (Ocelli et al., 1987; Chen et al., 1995), which would be an advantage in sorption and catalysis related processes where mass transfer is kinetically important (Ocelli et al., 1987).

\* Corresponding author.

E-mail address: [fanmd@imu.edu.cn](mailto:fanmd@imu.edu.cn) (M. Fan).



Scheme 1. Resonance structures of PVP molecule.

Reasonable adsorption of polymer on Mt is another way for forming the card-house structure, mainly through the adsorbed polymer layers induced steric repulsions between Mt particles (Alexandre and Dubois, 2000). As a water-soluble nonionic polymer with somewhat amphiphilic character, polyvinylpyrrolidone (PVP) exhibits a strong adsorption tendency to Mt from aqueous solution (Blum and Eberl, 2004), though the mechanism is still under discussion. The PVP molecule contains a hydrophobic polyvinyl backbone with pyrrolidone pendant groups (Scheme 1a), which in water has a resonance structure with electron-rich oxygen and electron-deficient nitrogen atoms (Scheme 1b). Such polarized nitrogen atoms and oxygen atoms can act as electron acceptors and donors respectively, and thus provide hydrophilic  $N^+ = C-O^-$  bonds in the PVP side rings (Sui et al., 2006). Based on the low measured displacement adsorption enthalpy ( $-1.6$  kJ/mol) of PVP on Mt surface, Séquaris et al. (2000) proposed a mechanism that the polymer is bound to Mt mainly through polar interaction between the positively charged nitrogen atoms and the negatively charged clay mineral surface. However, for the reason that in PVP molecule the oxygen atoms are less sterically hindered than the nitrogen atoms by the carbonic chains, another mechanism has also been suggested that the PVP adsorption on Mt mainly resorts to hydrogen bonding between the oxygen atoms and the clay mineral surface hydroxyl groups (Rao and Blanton, 2008). Governed by these possible mechanisms, well-defined PVP layers adsorbed on Mt have been observed in many works, where the conformational structures of the polymer layers are believed to depend on the molar mass and adsorbed amount of PVP; at the low molar mass and adsorbed amount, the polymer is mainly adsorbed through train segments, resulting in relatively thin PVP adsorbed layers, yet the high molar mass and adsorbed amount tend to give relatively thick PVP adsorbed layers in which extended loops and tails predominate (Séquaris et al., 2002; Blum and Eberl, 2004).

In many practices of producing metal nanoparticles by colloid-chemical methods, PVP has also been an efficient capping agent to tailor the size, shape, and dispersity of these nanoparticles (Koczur et al., 2015). This tailoring would be largely attributed to the binding affinities of PVP to the precursor metal ions and the subsequently formed nuclei and the further developed particles, making the growth processes of these metal nanoparticles under control. The affinity behaviors are commonly proposed to relate to the oxygen atoms rather than the nitrogen atoms of the polarized amide groups in PVP (Zhao et al., 2013). In the present study, we focused on the facile and controllable synthesis of metallic iron ( $Fe^0$ ) nanoparticles, dictated by the presence of Mt host (wherein a card-house structure is expected) and PVP stabilizer. Much attention in the past years has been paid to iron nanoparticles, for their novel property-dependent potentials in many practical applications (Huber, 2005; Li et al., 2006; Crane and Scott, 2012). To date, the chemical reduction of iron ions in solution by alkaline borohydrides has been widely used to prepare iron nanoparticles for its simplicity and security (Sun et al., 2006). With this method, the challenge from the oxidation of iron nanoparticles can be effectively circumvented by passivating them with iron oxide shells to preserve  $Fe^0$  phases (Bomatí-Miguel et al., 2006); and the challenge from the agglomeration of iron nanoparticles can be largely resolved by dispersing them in inorganic and/or organic protective colloids (such as Mt and PVP) (Sakulchaicharoen et al., 2010; Arancibia-Miranda et al.,

2016). Up to now, through the borohydride method although some groups have succeeded in synthesizing iron nanoparticles by employing Mt or PVP alone (Chen et al., 2011; Bhowmick et al., 2014), few studies as we know are available on synthesizing iron nanoparticles with both Mt and PVP involved. In this sense, taking advantage of the compatibility between Mt and PVP and their potentials to tune the growth process of iron nanoparticles, it is promising to achieve facile and controllable synthesis of iron nanoparticles by simultaneously introducing Mt and PVP into the borohydride reduction system.

Consequently, the objectives of this work were to in  $NaBH_4$  reduction systems synthesize  $Fe^0$ -Fe oxide core-shell nanoparticles hybridized with PVP-modified Mt particles (arranged in a card-house fashion), and to derive regulation parameters (such as the molar mass and concentration of PVP and the amount of  $NaBH_4$ ) for tailoring the size and dispersity of these iron nanoparticles. A combination of spectroscopic and microscopic techniques was used to obtain the microstructural information of the final products and to get insight into the mechanisms behind the card-house formation for the Mt host and the properties tailoring for the iron particles.

## 2. Materials and methods

### 2.1. Materials

The Mt used was sodium form (hereafter  $Na^+$ -Mt) from Zhejiang Sanding Technology Co., Ltd., China and the  $< 2 \mu m$  fraction was collected by sedimentation. Its cation exchange capacity was determined to be  $8.7 \times 10^{-4}$  eq/g. PVP with different molar masses 8000, 58,000, and 1,300,000 g/mol (Shanghai Aladdin Bio-Chem Technology Co., Ltd., China) and chemicals  $FeCl_3 \cdot 6H_2O$ ,  $NaBH_4$ , ethanol, and acetone (Shanghai Jiachen Chemical Co., Ltd., China) were of analytical grade and used as received. Deionized water was used throughout this work.

### 2.2. Preparation of samples

The iron nanoparticles hybridized with both Mt and PVP were synthesized by a borohydride reduction method. Typically,  $Na^+$ -Mt (2.0 g) was stirred in 100 mL of water for 24 h, and then PVP (molar mass 8000, 58,000, or 1,300,000 g/mol; amount 0.5, 2.0, or 4.0 g) was added to the aqueous clay mineral dispersion. The mixture was stirred for another 24 h and then 4.4 mmol  $FeCl_3 \cdot 6H_2O$  was added under stirring. After 24 h, 100 mL of freshly prepared  $NaBH_4$  solution (B/Fe molar ratio 4:1 or 6:1) was introduced dropwise into the system and kept stirring for 20 min. As the reducing agent was added the solution turned black indicating the reduction of ferric ions. The pH of the final solution was measured without any adjustment. All the experiments were carried out at ambient temperatures ( $\sim 25^\circ C$ ) and no precautions were taken to eliminate oxygen from the reaction vessels. The final products were washed thoroughly by centrifugation/redispersion cycles in 50 vol% aqueous ethanol solution then in anhydrous acetone, and then vacuum dried overnight at  $25^\circ C$ . Reference bare iron nanoparticles were prepared by the same procedure described above, except the absence of Mt and PVP.

### 2.3. Characterization

X-ray diffraction (XRD) patterns were recorded on a Bruker D8 Advance diffractometer using  $Cu K\alpha$  radiation (40 kV and 40 mA) and a position-sensitive detector (PSD). The scan mode of continuous PSD fast was selected at a counting time of 0.1 s per step. X-ray photoelectron spectroscopy (XPS) measurements were performed on a Thermo Scientific Escalab 250Xi system with 150 W monochromatic  $Al K\alpha$  radiation. The base pressure in the analysis chamber was about  $9.4 \times 10^{-10}$  mbar. For high-resolution spectra, constant analyzer energy mode was applied with a pass energy of 20 eV and step size of

Download English Version:

<https://daneshyari.com/en/article/5468598>

Download Persian Version:

<https://daneshyari.com/article/5468598>

[Daneshyari.com](https://daneshyari.com)